

MV-FAC: Mean–Variance Value Function Factorization for Multi-Robot Mean–Standard Deviation Moving Target Search

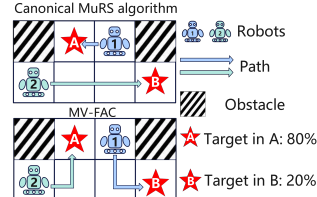
Anonymous Submission

Abstract

This paper studies a risk-sensitive formulation of the multi-robot search problem, termed multi-robot mean–standard deviation search (MuRMSS), in which a team of robots cooperatively search for a moving target by minimizing a linear combination of the mean and standard deviation of search time. However, the standard deviation term is inherently non-additive, making it difficult to estimate, incompatible with canonical multi-robot search algorithms, and preventing consistent decomposition into individual robot utilities, which is essential for scalable multi-robot cooperation. In view of these challenges, we propose MV-FAC, which comprises a mean–variance temporal-difference module that jointly learns the mean and variance of search time, a factorization module that decomposes them into individual utilities, and a decentralized policy optimization module that minimizes each robot’s individual mean–std objective. We further establish and prove the mean–std individual-global minimization (MS-IGM) theorem, thereby ensuring consistency between individual- and team-level objectives. Extensive simulation studies on standard multi-robot search benchmarks demonstrate that MV-FAC achieves the best overall mean–std search-time performance. We also validate MV-FAC’s practicality by deploying it on a physical multi-robot system for moving target search in a real-world building environment.

1 Introduction

Multi-robot search (MuRS) has long been an active research field, attracting sustained attention from both academia and industry. In practice, MuRS underpins a wide range of real-world applications, such as search and rescue in hazardous environments, persistent surveillance, and exploration in unknown environments. Beyond its practical relevance, MuRS also serves as a challenging and representative testbed for both algorithmic development and theoretical analysis in multi-agent systems, enabling the systematic study of core problems across multi-agent reinforcement learning, distributed control, and game-theoretic decision making.



(a) A Simple Scenario

Algorithms	Output	Mean+Std
Canonical MuRS Alg.	1→A 2→B	1.4+0.8 =2.2
MV-FAC	1→B 2→A	2+0 =2.0

(b) Performance Comparison

Figure 1: (a) A simple yet illustrative example of MuRMSS: two robots cooperate to search for one stationary target residing in Grid A with probability of 80% or in Grid B with probability of 20%, with the objective of minimizing the mean–std of search time. (b) Performance comparison: (1) Canonical MuRS algorithms dispatch Robot 1 to Grid A and Robot 2 to Grid B. The resulting mean search time is 1.4, with the variance 0.64, yielding a mean–std search time at $1.4 + \sqrt{0.64} = 2.2$. (2) MV-FAC dispatches Robot 1 to Grid B and Robot 2 to Grid A. The mean search time is 2, and the variance is 0, resulting in the mean–std search time at $2 + \sqrt{0} = 2$.

In the existing literature, multi-robot search has been studied under a variety of problem settings. Among them, a prevalent line of work focuses on minimizing the expected search time. While such expectation-based objectives are intuitive and convenient, they fail to capture the variability of search outcomes. In many risk-sensitive applications, it is preferable to sacrifice a small amount of expected search time for the reduced search-time variance. In view of these considerations, we introduce a risk-sensitive multi-robot search problem, termed multi-robot mean–standard deviation search (MuRMSS), which aims at minimizing the linear combination of mean and standard deviation (mean–std) search time.

However, MuRMSS alters the underlying problem structure, causing the canonical multi-robot search algorithms to yield suboptimal solutions. As illustrated in Fig. 1a, even in a simple scenario, algorithms designed to minimize the expected search time are no longer optimal under the mean–std search objective. Moreover, the standard-deviation term is inherently nonlinear and non-additive, which complicates its modeling and estimation procedure, and prevents the effective decomposition into individual robot utilities for decentralized decision making.

To address the aforementioned challenges, we propose mean–variance value function factorization (MV-FAC), a fac-

66 torized multi-agent reinforcement learning (MARL) method
67 for the MuRMSS problem. MV-FAC consists of (1) a mean-
68 variance temporal difference (TD) learning module, which
69 jointly estimates the team-level mean and variance of search
70 time, thereby circumventing the need to directly model the
71 non-additive standard-deviation term in MuRMSS; (2) a
72 mean-variance factorization module, which simultaneously
73 decomposes the team-level mean and variance into corre-
74 sponding individual-level utilities for each robot; and (3) a de-
75 centralized policy optimization module, which enables each
76 robot to update its decision-making policy towards minimiz-
77 ing the individual-level mean–std objective. Furthermore,
78 we establish the mean–std individual-global minimization
79 (MS-IGM) theorem, which guarantees consistency between
80 individual- and team-level mean–std objectives. We evaluate
81 MV-FAC against state-of-the-art methods on standard multi-
82 robot search benchmarks, and further validate its effectiveness
83 through deployment on a physical multi-robot system for
84 moving-target search in a real-world building environment.

85 The paper’s main contributions can be summarized as fol-
86 lows: (1) We formulate a risk-sensitive multi-robot search
87 problem, termed MuRMSS, which explicitly incorporates
88 both the mean and standard deviation into the search-time ob-
89 jective. (2) We propose MV-FAC for the MuRMSS problem,
90 which jointly learns and factorizes the team-level mean and
91 variance of search time into corresponding individual-level
92 utilities, thereby enabling decentralized policy optimization.
93 (3) We establish and prove the MS-IGM theorem, which
94 guarantees local-to-global consistency between individual-
95 and team-level mean–std objectives.

96 2 Literature Review

97 This section reviews related work on multi-robot search from
98 the perspectives of problem settings and solution method-
99 ologies, and further discusses representative studies on risk-
100 sensitive multi-agent decision making.

101 2.1 Problem Settings in Multi-Robot Search

102 Multi-robot search has been studied under various problem
103 settings, among which multi-robot efficient search (MuRES),
104 multi-robot adversarial search (MuRAS), and multi-robot
105 guaranteed search (MuRGS) are the most representative.

106 **1) Multi-robot efficient search (MuRES):** MuRES is the
107 most classical and widely studied problem setting in multi-
108 robot search. In this setting, the target is assumed to be non-
109 adversarial, *i.e.*, its motion dynamics are independent of the
110 robot team’s search strategy, and the objective is to mini-
111 mize the expected search time. Within the MuRES setting,
112 existing studies have explored a variety of modeling varia-
113 tions along several dimensions, including environment rep-
114 resentations such as grid-based [Lee and Lee, 2024], graph-
115 based [Patil *et al.*, 2023], and continuous environments [Kwa
116 *et al.*, 2020]; sensor characteristics such as perfect detec-
117 tion [Sheng *et al.*, 2022] and imperfect sensing with false neg-
118 atives [Asfora *et al.*, 2020] and/or false positives [Sun *et al.*,
119 2020]; sensing ranges including same-node detection [Guo *et
120 al.*, 2023a], neighbor-node detection [Chen *et al.*, 2024], and
121 line-of-sight sensing [Cui *et al.*, 2021]; and robot team com-

positions such as homogeneous robot teams [Andreychuk *et
122 al.*, 2025] and heterogeneous robot teams [Jo and Son, 2025].
123

124 **2) Multi-robot adversarial search (MuRAS):** MuRAS
125 extends the classical multi-robot search problem setting by
126 explicitly modeling the target as an adversarial one, which
127 acts adversarially against the robot team’s search strat-
128 egy [Rahman *et al.*, 2022; Peng *et al.*, 2025a]. In this set-
129 ting, the robot team still aims to minimize the expected search
130 time, however, the target actively attempts to evade the robots
131 in order to delay detection. Due to the adversarial nature of
132 target motion, MuRAS is often studied under the pursuit-
133 evasion framework [Fang *et al.*, 2022; Olsen *et al.*, 2022].
134

135 **3) Multi-robot guaranteed search (MuRGS):** MuRGS
136 considers a more conservative problem setting in which the
137 robot team seeks to guarantee target detection without making
138 assumptions about the target’s motion characteristics [Kolling
139 and Kleiner, 2013]. Unlike MuRES and MuRAS, MuRGS
140 typically adopts the worst-case performance criterion, aiming
141 to minimize the maximum possible search time regardless of
142 the target’s motion behavior and initial location. As a result,
143 MuRGS is commonly studied in settings where safety-critical
144 requirements necessitate strict upper bounds on search time.
145

146 This paper introduces MuRMSS, which defines a differ-
147 ent problem setting from MuRES, MuRAS and MuRGS.
148 MuRMSS follows the non-adversarial moving target assump-
149 tion in MuRES, but departs from the existing formulations by
150 adopting a risk-sensitive objective that minimizes the mean-
151 standard deviation of search time. The risk-sensitive objec-
152 tive introduces additional challenges due to the non-additivity
153 of the standard-deviation term, making classical multi-robot
154 search methods insufficient for the problem setting.
155

156 2.2 Methodologies for Multi-Robot Search

157 Existing methodologies for multi-robot search can be broadly
158 categorized into four groups: planning-based methods, swarm
159 intelligence methods, game-theoretic methods, and multi-
160 agent reinforcement learning (MARL)-based methods.
161

162 **1) Planning-based methods** represent the most canon-
163 ical solutions for the MuRES problem. They typically for-
164 mulate multi-robot search as a mathematical optimization
165 problem by explicitly modeling target motion, initial lo-
166 cation uncertainty, and robot dynamics, and solve it us-
167 ing off-the-shelf optimization solvers [Asfora *et al.*, 2020;
168 Gonzalez and Jaillet, 2025; Shree *et al.*, 2021]. However,
169 these methods suffer from poor scalability, as the computa-
170 tional complexity grows rapidly with the number of robots,
171 target uncertainty, and environment size.
172

173 **2) Swarm intelligence methods** address the multi-robot
174 search problem by prescribing simple local behavior or
175 interaction rules for individual robots, from which team-
176 level search behaviors emerge through decentralized execu-
177 tion [Yuan *et al.*, 2024; Sharma *et al.*, 2025; Morin *et al.*,
178 2022]. While intuitive, easy to implement, and highly scal-
179 able, they lack an explicit objective-driven problem formula-
177 tion, making it difficult to relate local rules to the global ob-
178 jective and systematically optimize team-level performance.
179

177 **3) Game-theoretic methods** model multi-robot search as
178 an interactive decision-making process between the robot
179 team and an adversarially moving target, and typically formu-
179

late the problem within the zero-sum or pursuit–evasion game framework to seek equilibrium-based solutions [Zhou *et al.*, 2024b; Esfahani *et al.*, 2026] or derive sufficient conditions for guaranteed search success [Bone *et al.*, 2023]. However, such methods often rely on restrictive assumptions about the target’s capabilities and/or environment properties, and face scalability challenges in complex settings.

4) MARL-based methods have recently emerged as a promising approach for the MuRES problem by formulating multi-robot search as a decentralized sequential decision-making process [Calzolari *et al.*, 2025; Tan *et al.*, 2021; Hou *et al.*, 2024; Zhou *et al.*, 2024a]. These methods typically cast MuRES within the decentralized partially observable Markov decision process (Dec-POMDP) framework and employ distributed policy optimization algorithms, such as multi-agent policy gradient [Chen *et al.*, 2025; Guo *et al.*, 2023a] or value-function factorization [Guo *et al.*, 2025], to learn cooperative search strategies from the interaction data.

2.3 Risk-Sensitive Multi-Agent Decision Making

Risk-sensitive multi-agent decision making has recently attracted increasing attention, aiming to extend beyond canonical expectation-based objectives by explicitly accounting for uncertainty and variability in long-term returns. Representative studies focus on distribution-based risk measures, such as value-at-risk (VaR), conditional value-at-risk (CVaR), and distortion risk measures (DRMs), and develop corresponding value factorization frameworks to enable decentralized execution under these risk-sensitive objectives [Slumbers *et al.*, 2022; Gao *et al.*, 2021; Shen *et al.*, 2023; Jiang *et al.*, 2025]. In this context, it has been shown that classical expectation-based IGM principles are generally insufficient, motivating generalized consistency conditions and quantile-based factorization architectures for non-additive risk operators.

Despite the progress, existing risk-sensitive multi-agent decision-making methods primarily target distributional risk objectives, which require learning and manipulating the *full* return distribution and tend to incur substantial computational complexity. In contrast, the MuRMSS problem adopts a mean–standard deviation objective, where risk sensitivity is characterized by first- and second-order statistics rather than full distributional modeling, motivating a more lightweight algorithmic design that only estimates and factorizes the mean and variance of search time. A detailed review of risk-sensitive MARL is presented in the supplementary material.

3 Problem Formulation

This section presents the problem formulation of MuRMSS and its modeling within the decentralized partially observable Markov decision process (Dec-POMDP) framework. For clarity, a summary of major notations used throughout the paper is provided in the supplementary material.

3.1 Task-Level Problem Definition

The task-level definition of MuRMSS specifies the operating environment, the target motion dynamics, the robots’ sensing and motion models, and the target detection condition.

1) Operating Environment: The environment is modeled as an undirected and connected unit-cost graph $\mathcal{G}(\mathcal{V}, \mathcal{E})$,

where \mathcal{V} denotes the set of nodes, and \mathcal{E} denotes the set of edges. The unit-cost assumption means that traversing any edge or remaining at the same node incurs one time step for both the robots and the target. This assumption has been commonly adopted in the multi-robot search literature for discrete environments, see [Guo *et al.*, 2025; Asfora *et al.*, 2020; Sheng *et al.*, 2022] as examples. In practice, non-unit-cost graphs can be converted into unit-cost ones by subdividing long edges into several unit-cost sub-edges.

2) Target Motion Dynamics: The target’s position at time step t is denoted by $e_t \in \mathcal{V}$, and is unknown to the robot team. The target’s motion is assumed to be non-adversarial, meaning that the motion dynamics are *independent* of the robot team’s search strategy. The target motion is modeled as a discrete-time Markov process governed by the stochastic transition matrix Γ , *i.e.*, $\mathbb{P}[e_{t+1}|e_t] = \Gamma(e_t, e_{t+1})$. Here, Γ respects the underlying graph \mathcal{G} , such that $e_{t+1} = e_t$ or $(e_t, e_{t+1}) \in \mathcal{E}$, and is also unknown to the robot team.

3) Robot Model: We consider a team of N robots indexed by $i \in \{1, \dots, N\}$. Robot i ’s position at time step t is denoted by $p_t^{(i)} \in \mathcal{V}$, and at each time step, robot i can either move to an adjacent node in \mathcal{G} , *i.e.*, $(p_t^{(i)}, p_{t+1}^{(i)}) \in \mathcal{E}$ or remain stationary at the current node, *i.e.*, $p_{t+1}^{(i)} = p_t^{(i)}$. Each robot is equipped with a local sensor and receives a binary observation $o_t^{(i)} \in \{0, 1\}$, where $o_t^{(i)} = 1$ indicates that the target is detected at node $p_t^{(i)}$, while $o_t^{(i)} = 0$ for no target detection at node $p_t^{(i)}$. The decision-making policy of robot i , denoted by $\pi^{(i)}$, depends on its own history of positions and observations, *i.e.*, $\pi^{(i)} = \pi^{(i)}(p_{\leq t}^{(i)}, o_{\leq t}^{(i)})$.

4) Target Detection Condition: The target is deemed to be detected if, at any time step t , there exists at least one robot i such that the robot and the target reside at the same node, *i.e.*, $p_t^{(i)} = e_t$. The time step at which this event first occurs is defined as the search time and is denoted by t_{cap} . Here, t_{cap} is a random variable due to the stochastic target motion and the uncertainty in the target’s initial location.

3.2 Dec-POMDP Modeling for MuRMSS

Based on the task-level definition in Section 3.1, we formulate MuRMSS as a decentralized partially observable Markov decision process (Dec-POMDP). A Dec-POMDP is defined by the tuple $\langle \mathcal{I}, \mathcal{S}, \{\mathcal{A}^{(i)}\}, \{\mathcal{O}^{(i)}\}, \mathbb{P}, R, \gamma \rangle$, and each element is specified within the multi-robot search context.

The set of agents is given by $\mathcal{I} = \{1, \dots, N\}$, where N is the number of searching robots. The global state $s_t \in \mathcal{S}$ is defined as the joint configuration of the target and all robots at time t , *i.e.*, $s_t = (e_t, p_t^{(1)}, \dots, p_t^{(N)})$. Each robot $i \in \mathcal{I}$ selects an action $a_t^{(i)} \in \mathcal{A}^{(i)}$, which corresponds to moving to one of the neighboring nodes or remaining stationary, yielding the joint action $\mathbf{a}_t = (a_t^{(1)}, \dots, a_t^{(N)})$. Each robot i receives a local observation $o_t^{(i)} \in \{0, 1\}$, indicating whether the target is detected at its current node. Each robot follows a decentralized policy $\pi^{(i)}$ based on its local position-observation history.

The state transition function \mathbb{P} is induced by the robots’

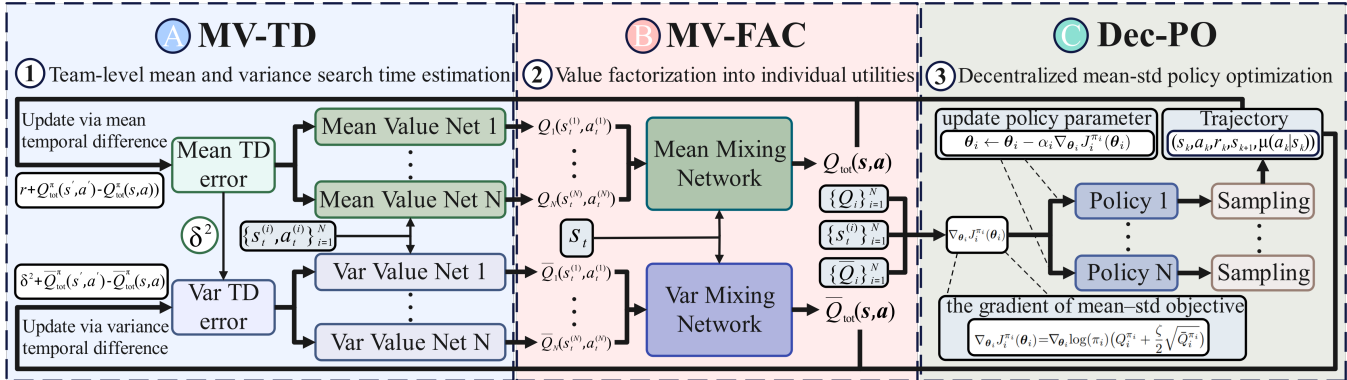


Figure 2: The MV-FAC Framework: (A) MV-TD estimates the team-level mean and variance value functions of search time; (B) MV-FAC decomposes the team-level mean and variance value functions into individual-level utilities with the monotonic mixing networks; and (3) Dec-PO updates each robot’s decision-making policy based on the mean–std policy gradient.

joint actions and the target’s stochastic motion dynamics. Robot motion is deterministic given the action and graph connectivity, whereas the target motion is stochastic and independent of the robots’ behavior. The instantaneous reward r_t is set to 1 at each time step until termination, corresponding to the unit time cost. We consider an undiscounted episodic setting with $\gamma = 1$, under which the cumulative return equals t_{cap} . Unlike standard expectation-based formulations, MuRMSS adopts a risk-sensitive objective that minimizes the mean–standard deviation of t_{cap} under the joint policy π , *i.e.*, $\min_{\pi} \mu(t_{\text{cap}}) + \zeta \sigma(t_{\text{cap}})$, where $\mu(t_{\text{cap}})$ and $\sigma(t_{\text{cap}})$ denote the mean and standard deviation of t_{cap} , respectively, and $\zeta > 0$ is a risk-sensitivity coefficient.

4 The MV-FAC Framework

This section presents the mean–variance value function factorization (MV-FAC) framework to solve the MuRMSS problem. Unlike the distributional risk-sensitive MARL methods designed for VaR-, CVaR-, or distortion-based objectives, MV-FAC directly targets the mean–std objective by estimating and factorizing only the mean and variance of search time, resulting in a lightweight and scalable design.

The MV-FAC framework consists of three coupled components that form an ‘estimation-factorization-optimization’ loop: (1) a mean–variance temporal difference (MV-TD) module that *estimates* the mean and variance of search time under a given joint policy; (2) a mean–variance value function factorization (MV-FAC) module that *factorizes* the team-level mean and variance into individual utilities; and (3) a decentralized policy optimization (Dec-PO) module that *optimizes* each robot’s policy based on the factorized mean–variance objective. We further provide MV-FAC’s pseudocode along with its computational complexity analysis. An overview of the MV-FAC framework is presented in Fig. 2.

4.1 Mean–Variance Temporal Difference (MV-TD)

The MV-TD module estimates the mean and variance of search time under a given joint policy π by extending standard TD learning to the use case of second-order statistics. We first introduce the mean–variance Bellman equation set,

and then present the corresponding TD methods for online model-free estimation of these quantities.

The team-level mean action-value function $Q_{\text{tot}}^{\pi}(s, a)$, which corresponds to the expected search time when taking the joint action a at global state s , under policy π satisfies the following *mean* Bellman equation:

$$Q_{\text{tot}}^{\pi}(s, a) = \sum_{s' \in \mathcal{S}} \mathbb{P}(s'|s, a) \left[r(s, a, s') + \mathbb{E}_{\pi} Q_{\text{tot}}^{\pi}(s', a') \right]. \quad (1)$$

Correspondingly, the team-level variance action-value function $\bar{Q}_{\text{tot}}^{\pi}(s, a)$, satisfies the *variance* Bellman equation:

$$\bar{Q}_{\text{tot}}^{\pi}(s, a) = \sum_{s' \in \mathcal{S}} \mathbb{P}(s'|s, a) \sum_{a' \in \mathcal{A}} \pi(a'|s') [\delta^2 + \bar{Q}_{\text{tot}}^{\pi}(s', a')], \quad (2)$$

where $\delta = r(s, a, s') + Q_{\text{tot}}^{\pi}(s', a') - Q_{\text{tot}}^{\pi}(s, a)$ refers to the sampled TD error. Note that the derivation process of the variance Bellman equation (Eq. (2)) makes use of the law of total variance in probability theory, and is presented in the supplementary material.

The mean–variance Bellman equation set, *i.e.*, Eq. (1) and Eq. (2), provides the theoretical foundation for estimating the mean and variance of the return. Building on this foundation, we develop the mean–variance temporal difference (MV-TD) method to estimate these quantities in an online, model-free manner. Given a transition tuple $\langle s, a, r, s', a' \rangle$ sampled according to the joint policy π , the estimates of $Q_{\text{tot}}^{\pi}(s, a)$ and $\bar{Q}_{\text{tot}}^{\pi}(s, a)$ are recursively updated as follows:

$$Q_{\text{tot}}^{\pi}(s, a) \leftarrow Q_{\text{tot}}^{\pi}(s, a) + \alpha (r + Q_{\text{tot}}^{\pi}(s', a') - Q_{\text{tot}}^{\pi}(s, a)) \quad (3)$$

$$\bar{Q}_{\text{tot}}^{\pi}(s, a) \leftarrow \bar{Q}_{\text{tot}}^{\pi}(s, a) + \bar{\alpha} (\delta^2 + \bar{Q}_{\text{tot}}^{\pi}(s', a') - \bar{Q}_{\text{tot}}^{\pi}(s, a)), \quad (4)$$

where α and $\bar{\alpha}$ are the step-size parameters for the mean and variance value functions, respectively.

Note that both the mean–variance Bellman equations (Eqs. (1)–(2)) and the corresponding mean–variance TD updates (Eqs. (3)–(4)) are formulated primarily for estimating the team-level *action*-value functions, *i.e.*, $Q_{\text{tot}}^{\pi}(s, a)$ and $\bar{Q}_{\text{tot}}^{\pi}(s, a)$. In practice, these formulations can be naturally adapted with minor modifications to estimate the corresponding *state*-value functions, *i.e.*, $V_{\text{tot}}^{\pi}(s)$ and $\bar{V}_{\text{tot}}^{\pi}(s)$, as detailed in the supplementary material.

4.2 Mean–Variance Factorization (MV-FAC)

MV-TD estimates the team-level mean and variance value functions, which characterize the expected search time and its variation. However, scalable multi-robot coordination requires further decomposing these quantities into individual utilities to support decentralized policy optimization. We next introduce the mean–variance value function factorization (MV-FAC) module.

MV-FAC employs two parallel factorization architectures to decompose team-level value functions into individual utilities. Specifically, a *mean factorization network* decomposes the team-level mean action-value function ($Q_{\text{tot}}^{\pi}(s, a)$) into individual-level mean action-value functions ($Q_i^{\pi_i}(s_i, a_i)$), while a *variance factorization network* decomposes the team-level variance action-value function ($\bar{Q}_{\text{tot}}^{\pi}(s, a)$) into individual-level variance action-value functions ($\bar{Q}_i^{\pi_i}(s_i, a_i)$). Each factorization network consists of agent-specific utility networks, and a mixing network whose parameters are generated by state-conditioned hyper-networks. The hyper-networks enforce non-negative mixing weights, guaranteeing the following monotonicity conditions:

$$\frac{\partial Q_{\text{tot}}^{\pi}(s, \mathbf{a})}{\partial Q_i^{\pi_i}(s_i, a_i)} \geq 0, \quad \frac{\partial \bar{Q}_{\text{tot}}^{\pi}(s, \mathbf{a})}{\partial \bar{Q}_i^{\pi_i}(s_i, a_i)} \geq 0, \quad \forall i \in \mathcal{I}. \quad (5)$$

Based on these monotonicity conditions, we establish the mean–std individual-global minimization (MS-IGM) theorem that ensures consistency between individual- and team-level mean–std objectives.

Theorem 1 (The MS-IGM Theorem). *Suppose that the team-level mean and variance action-value functions admit monotonic factorizations with respect to corresponding individual utilities. Then, $\forall \zeta > 0$, the greedy minimization of the team-level mean–std objective is consistent with that of the individual-level objectives, i.e.,*

$$\begin{aligned} & \arg \min_{\mathbf{a}} \left(Q_{\text{tot}}^{\pi}(s, \mathbf{a}) + \zeta \sqrt{\bar{Q}_{\text{tot}}^{\pi}(s, \mathbf{a})} \right) \\ &= \left(\begin{array}{c} \arg \min_{a_1} Q_1^{\pi_1}(s_1, a_1) + \zeta \sqrt{\bar{Q}_1^{\pi_1}(s_1, a_1)} \\ \vdots \\ \arg \min_{a_N} Q_N^{\pi_N}(s_N, a_N) + \zeta \sqrt{\bar{Q}_N^{\pi_N}(s_N, a_N)} \end{array} \right). \end{aligned} \quad (6)$$

Proof.

$$\begin{aligned} & \frac{\partial(Q_{\text{tot}} + \zeta \sqrt{\bar{Q}_{\text{tot}}})}{\partial(Q_i + \zeta \sqrt{\bar{Q}_i})} \\ &= \frac{\partial Q_{\text{tot}}}{\partial Q_i} \cdot \frac{\partial Q_i}{\partial(Q_i + \zeta \sqrt{\bar{Q}_i})} + \frac{\partial(\zeta \sqrt{\bar{Q}_{\text{tot}}})}{\partial \bar{Q}_i} \cdot \frac{\partial \bar{Q}_i}{\partial(Q_i + \zeta \sqrt{\bar{Q}_i})} \\ &= \frac{\partial Q_{\text{tot}}}{\partial Q_i} \cdot \frac{\partial Q_i}{\partial(Q_i + \zeta \sqrt{\bar{Q}_i})} + \frac{\zeta}{2\sqrt{\bar{Q}_{\text{tot}}}} \cdot \frac{\partial \bar{Q}_{\text{tot}}}{\partial \bar{Q}_i} \cdot \frac{\partial \bar{Q}_i}{\partial(Q_i + \zeta \sqrt{\bar{Q}_i})} \\ &= \frac{\partial Q_{\text{tot}}}{\partial Q_i} \cdot \frac{1}{1 + \zeta \cdot \frac{\partial \sqrt{\bar{Q}_i}}{\partial Q_i}} + \frac{\zeta}{2\sqrt{\bar{Q}_{\text{tot}}}} \cdot \frac{\partial \bar{Q}_{\text{tot}}}{\partial \bar{Q}_i} \cdot \frac{1}{\zeta \cdot \frac{\partial \sqrt{\bar{Q}_i}}{\partial Q_i}} \\ &= \frac{\partial Q_{\text{tot}}}{\partial Q_i} + \frac{\sqrt{\bar{Q}_i}}{\sqrt{\bar{Q}_{\text{tot}}}} \cdot \frac{\partial \bar{Q}_{\text{tot}}}{\partial \bar{Q}_i} \geq 0. \end{aligned}$$

□

Note that in the above proof process, we omit the superscripts π and π_i , and (s_i, a_i) for notational brevity, and make use of the independence between the mean and variance factorization processes, *i.e.*, $\partial Q_{\text{tot}}/\partial \bar{Q}_i = 0$, $\partial \bar{Q}_{\text{tot}}/\partial Q_i = 0$.

4.3 Decentralized Policy Optimization (Dec-PO)

The MS-IGM theorem established in Section 4.2 ensures that minimizing individual mean–standard deviation utilities is consistent with optimizing the team-level objective. In this subsection, we present the decentralized policy optimization (Dec-PO) module, which updates each robot’s policy using only its own factorized mean–variance value functions.

Defining the individual-level mean–std objective as $J_i^{\pi_i} = Q_i^{\pi_i} + \zeta \sqrt{\bar{Q}_i^{\pi_i}}$, we derive its gradient with respect to the policy parameters θ_i , which is used for decentralized policy optimization.

$$\begin{aligned} & \nabla_{\theta_i} J_i^{\pi_i}(\theta_i) \\ &= \nabla_{\theta_i} (Q_i^{\pi_i} + \zeta \sqrt{\bar{Q}_i^{\pi_i}}) \\ &= \nabla_{\theta_i} Q_i^{\pi_i} + \zeta \nabla_{\theta_i} \sqrt{\bar{Q}_i^{\pi_i}} \\ &= \nabla_{\theta_i} Q_i^{\pi_i} + \frac{\zeta}{2\sqrt{Q_i^{\pi_i}}} \nabla_{\theta_i} \bar{Q}_i^{\pi_i} \\ &\stackrel{(*)}{\approx} (\nabla_{\theta_i} \log \pi_i) \times Q_i^{\pi_i} + \frac{\zeta}{2\sqrt{Q_i^{\pi_i}}} (\nabla_{\theta_i} \log \pi_i) \times \bar{Q}_i^{\pi_i} \\ &= \nabla_{\theta_i} \log(\pi_i) \left(Q_i^{\pi_i} + \frac{\zeta}{2} \sqrt{\bar{Q}_i^{\pi_i}} \right), \end{aligned} \quad (7)$$

where $(*)$ follows from the canonical policy gradient theorem whose proof is provided in [Sutton and Barto, 2018]. Note that the symbol ‘ \approx ’ means *approximately proportional to*, and the final result in Eq. (7) is a stochastic approximation of the *true* gradient of $J_i^{\pi_i}(\theta_i)$. The above derivation process omits (s_i, a_i) for notational brevity, *e.g.*, $Q_i^{\pi_i}$ abbreviates $Q_i^{\pi_i}(s_i, a_i)$, and $\log(\pi_i)$ abbreviates $\log \pi_i(s_i, a_i)$.

With the derived gradient of $J_i^{\pi_i}(\theta_i)$ in Eq. (7), the Dec-PO module updates the individual robot’s policy network parameter vector θ_i as:

$$\theta_i \leftarrow \theta_i - \alpha_i \nabla_{\theta_i} J_i^{\pi_i}(\theta_i), \quad (8)$$

where $0 < \alpha_i < 1$ is the learning rate for the decentralized policy optimization process of Robot i .

4.4 Computational Complexity Analysis

In this subsection, we summarize the training procedure of the MV-FAC framework and analyze its computational complexity. Before presenting the pseudocode, we briefly introduce the notations used to describe the learnable components and optimization variables in MV-FAC. The parameter vectors of the individual mean and variance action-value networks, Q_i^{π} and \bar{Q}_i^{π} , are denoted by w_i and \bar{w}_i , respectively. Robot i ’s decision-making policy π_i is parameterized by θ_i . The parameters of the mean and variance hyper-networks are denoted by ϕ and $\bar{\phi}$, respectively.

The pseudocode of MV-FAC’s training procedure is presented in Algorithm 1, followed by the computational complexity analysis under the Big-O convention [Knuth, 1976].

Algorithm 1: MV-FAC’s Training Procedure

```

Input: (1) Graph  $\mathcal{G}(\mathcal{V}, \mathcal{E})$ ; (2) Risk Coefficient  $\zeta$ ;  

(3) # of Robots  $N$ ; (4) Max. # of Episodes:  $E_{\max}$ .  

Output: Decentralized policies  $\{\pi_i(\cdot | s_i; \theta_i)\}_{i \in \mathcal{I}}$ .
1 Initialize:
2 (1) Individual mean and variance action-value network  

parameters:  $\{w_i, \bar{w}_i\}_{i \in \mathcal{I}}$ ;  

3 (2) Individual policy network parameters  $\{\theta_i\}_{i \in \mathcal{I}}$ ;  

4 (3) Hyper-network parameters  $\phi$  and  $\bar{\phi}$ .  

5 (4) Replay buffer  $\mathcal{D} = \{\}$ ; counter  $\leftarrow 0$ ;  

6 while  $counter \leq E_{\max}$  do  

7   Reset environment;  $t \leftarrow 0$ ;  

8    $\forall i \in \mathcal{I}: s_i(t) \leftarrow 0, o_0^{(i)} \leftarrow 0$ ;  

9   while  $\forall i \in \mathcal{I}: o_t^{(i)} = 0$  do  

10    for each robot  $i \in \mathcal{I}$  do  

11      Observe  $(p_t^{(i)}, o_t^{(i)})$ ;  

12       $s_t^{(i)} \leftarrow \text{GRU}(s_{t-1}^{(i)}, p_t^{(i)}, o_t^{(i)})$ ;  

13      Sample  $a_t^{(i)} \sim \pi_i(a|s_t^{(i)})$ ;  

14      Execute joint action  $\mathbf{a}_t = \{a_t^{(i)}\}_{i \in \mathcal{I}}$ ;  

15       $r_t \leftarrow 1$ ;  

16      for each robot  $i \in \mathcal{I}$  do  

17        Observe  $(p_{t+1}^{(i)}, o_{t+1}^{(i)})$ ;  

18         $s_{t+1}^{(i)} \leftarrow \text{GRU}(s_t^{(i)}, p_{t+1}^{(i)}, o_{t+1}^{(i)})$ ;  

19        Store  $\langle \{s_t^{(i)}\}, \{a_t^{(i)}\}, r_t, \{s_{t+1}^{(i)}\} \rangle$  into  $\mathcal{D}$ ;  

20         $t \leftarrow t + 1$ .  

// MV-TD with MV-FAC  

21 Sample a mini-batch of transitions from  $\mathcal{D}$ ;  

22 for each robot  $i \in \mathcal{I}$  do  

23   Compute  $Q_i(s_i, a_i; w_i)$  and  $\bar{Q}_i(s_i, a_i; \bar{w}_i)$ ;  

24 Mix individual utilities with hyper-networks to  

obtain  $Q_{\text{tot}}(s, a)$  and  $\bar{Q}_{\text{tot}}(s, a)$ ;  

25 Calculate mean and variance TD errors:  $\delta$  and  $\bar{\delta}$ ;  

26 Update  $\{w_i, \bar{w}_i, \phi, \bar{\phi}\}$  to min.  $\sum \delta^2$  and  $\sum \bar{\delta}^2$ .  

// Dec-PO  

27 for each robot  $i \in \mathcal{I}$  do  

28   Update policy parameter  $\theta_i$  using Eq. (8) with  

 $Q_i(s_i, a_i)$  and  $\bar{Q}_i(s_i, a_i)$ .  

29 counter  $\leftarrow$  counter +1;

```

5 Simulation Results and Analysis

445
446
447
448
449
450
451
452
453
454
455
456
457
458

This section evaluates the proposed MV-FAC framework on standard multi-robot search (MuRS) benchmarks by comparing its mean–std performance with state-of-the-art baselines. The benchmark algorithms, summarized in Table I, span three representative categories: prevailing MuRS methods, canonical MARL algorithms, and risk-sensitive decision-making approaches. All baselines are adapted to the MuRMSS setting with identical observation and action spaces to ensure fair comparison. We further conduct an ablation study to systematically isolate and quantify the contribution of each module in MV-FAC. All meta-parameter configurations and additional experimental results are provided in the supplementary material, and the source code is publicly available¹.

Table I: Summary of Selected Baseline Algorithms

Category	Methodology
MuRS Methods	PF-MAAC [Peng <i>et al.</i> , 2025b] HMA-SAR [Cao <i>et al.</i> , 2024] CE-PG [Guo <i>et al.</i> , 2023a] DRL-Searcher [Guo <i>et al.</i> , 2023b]
MARL Algorithms	P-MAT [Hu <i>et al.</i> , 2025] HAPPO [Kuba <i>et al.</i> , 2022] QMIX [Rashid <i>et al.</i> , 2020]
Risk-Sensitive Approaches	RiskQ [Shen <i>et al.</i> , 2023] RMIX [Qiu <i>et al.</i> , 2021] D-FAC [Sun <i>et al.</i> , 2021]

5.1 Benchmark Comparison

This subsection evaluates MV-FAC against state-of-the-art baselines in terms of mean–std search-time performance on two standard multi-robot search (MuRS) benchmarks, MUSEUM and OFFICE (Fig. 3). In both environments, robots start from fixed initial nodes, *i.e.*, Node 1 in MUSEUM and Node 43 in OFFICE, while the target is randomly initialized over the environment. At each time step, the target moves non-adversarially to one of its adjacent nodes with equal probability, and is considered ‘detected’ when any robot occupies the same node as the target.

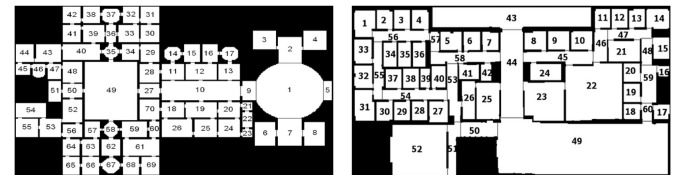


Figure 3: Standard MuRS benchmarks: MUSEUM and OFFICE.

Table II reports the mean–std performance comparison between MV-FAC and state-of-the-art baselines across different experimental configurations, including varying team sizes ($N \in \{3, 4, 5\}$) and risk-sensitivity coefficients ($\zeta \in \{0.1, 1, 10\}$). For each setting, results are obtained from 1000 independent simulation runs, with the sample mean and std to evaluate each algorithm’s final mean–std performance.

¹<https://anonymous.4open.science/r/MV-FAC-3D4F>.

433 Let B be the mini-batch size, and denote C_Q , $C_{\bar{Q}}$, C_{π} ,
434 C_{mix} as the unit cost of one forward/backward pass for in-
435 dividual mean/variance network (Q_i and \bar{Q}_i), individual pol-
436 icy network (π_i), and the mixing network, respectively. Per
437 episode, MV-TD evaluates N individual utilities, and applies
438 two mixing networks, yielding $\mathcal{O}(BN)$ forward/backward
439 passes, *i.e.*, $\mathcal{O}(BN(C_Q + C_{\bar{Q}}) + 2C_{\text{mix}})$. For Dec-PO, each
440 policy update costs $\mathcal{O}(BNC_{\pi})$. Therefore, the overall com-
441 plexity over E_{\max} episodes is $\mathcal{O}(E_{\max}(BN(C_Q + C_{\bar{Q}} +$
442 $C_{\pi}) + 2C_{\text{mix}}))$. Note that C_Q , $C_{\bar{Q}}$, C_{π} and C_{mix} depend on
443 the network configuration and the graph size, *i.e.*, $|\mathcal{V}|$ and $|\mathcal{E}|$.
444 Detailed analysis is provided in the supplementary material.

470
471
472
473
474
475
476

Table II: Performance comparison between MV-FAC and baseline algorithms on standard multi-robot search benchmarks. **Bold** numbers indicate the best mean–std performance, and underlined numbers indicate the second best performance.

Env.	N	ζ	MV-FAC	QMIX	D-FAC	PF-MAAC	HMA-SAR	CE-PG	DRL-Searcher	P-MAT	HAPPO	RiskQ	RMIX
OFFICE	3	0.1	5.18	6.09	7.13	7.55	7.27	9.85	7.43	6.45	6.92	<u>5.85</u>	6.12
		1.0	8.06	11.11	14.46	12.80	<u>10.33</u>	17.20	14.97	10.85	12.15	<u>10.45</u>	10.92
		10.0	36.86	61.33	87.72	75.40	<u>40.93</u>	92.15	90.39	55.20	68.30	<u>39.50</u>	41.20
	4	0.1	4.84	5.81	6.85	7.15	6.90	8.90	6.85	6.10	6.55	<u>5.25</u>	5.60
		1.0	7.16	9.97	13.20	11.50	9.80	16.50	12.66	10.15	11.80	<u>8.82</u>	9.45
		10.0	30.38	51.55	78.62	65.10	38.50	88.40	75.72	48.30	60.25	<u>35.15</u>	37.80
	5	0.1	4.68	5.34	6.42	6.90	6.55	8.15	6.42	5.60	6.20	<u>5.15</u>	5.28
		1.0	6.58	9.19	11.92	10.50	9.10	14.20	11.13	9.45	11.10	<u>8.25</u>	8.65
		10.0	25.57	47.71	69.89	58.40	35.20	75.60	66.21	42.50	55.80	<u>32.60</u>	34.25
MUSEUM	3	0.1	<u>6.55</u>	8.07	14.74	10.50	6.24	12.80	7.39	7.10	9.20	6.57	6.95
		1.0	9.44	14.30	23.50	18.40	<u>9.36</u>	21.50	12.83	11.20	15.60	9.55	9.88
		10.0	39.10	76.58	111.07	95.20	40.59	105.30	67.19	58.40	82.10	<u>38.15</u>	40.95
	4	0.1	5.95	7.50	12.25	9.10	<u>6.05</u>	11.40	7.13	6.95	8.50	6.30	6.65
		1.0	8.97	12.18	19.05	16.80	<u>9.10</u>	18.20	12.30	10.90	13.50	9.25	9.60
		10.0	37.97	65.28	95.09	82.50	38.41	95.60	64.05	55.20	68.40	<u>35.60</u>	38.30
	5	0.1	5.45	6.83	10.25	7.90	<u>5.80</u>	9.80	7.06	6.75	7.50	6.10	6.45
		1.0	8.39	11.04	16.10	14.50	<u>8.85</u>	15.40	11.81	10.55	12.40	8.95	9.15
		10.0	29.86	58.15	80.62	72.20	36.69	72.10	59.33	52.10	62.50	<u>33.86</u>	35.80

477 In Table II, we observe that (1) MV-FAC consistently
478 achieves the best or second-best mean–std performance
479 across all configurations, demonstrating strong robustness
480 to variations in both team size and risk sensitivity coefficient;
481 (2) the performance gap between MV-FAC and base-
482 line algorithms becomes increasingly pronounced as ζ grows,
483 highlighting MV-FAC’s ability to trade off expectation and
484 variability. In contrast, canonical MuRS and MARL algo-
485 rithms exhibit limited adaptability to high risk-sensitive sce-
486 narios. (3) While some risk-sensitive baselines, *e.g.*, RiskQ
487 and RMIX, also improve performance for larger ζ values,
488 their gains are generally inconsistent across different team
489 sizes², whereas MV-FAC maintains stable and scalable per-
490 formance as the team size grows.

491 5.2 Ablation Study

492 This subsection conducts an ablation study to isolate the con-
493 tribution of each module in MV-FAC. Specifically, we com-
494 pare four variants: (1) I-MV-TD (ϵ), where each robot inde-
495 pendently learns its own mean–variance value functions via
496 MV-TD and selects actions using the ϵ -greedy policy; (2) I-
497 MV-TD (Dec), which replaces ϵ -greedy with the Dec-PO pol-
498 icy update process; (3) MV-TD+MV-FAC (ϵ), which learns
499 team-level mean and variance values and applies MV-FAC to
500 decompose them into individual utilities, but uses ϵ -greedy
501 for action selection; (4) MV-TD+MV-FAC+Dec-PO, the full
502 MV-FAC framework that couples MV-TD estimation, MV-
503 FAC factorization, and Dec-PO optimization.

504 Table III presents the comparative mean–std performance
505 of the four MV-FAC variants in the OFFICE environment. We
506 observe that I-MV-TD(ϵ) shows limited improvement with
507 increasing team size, as independent ϵ -greedy policies lead
508 to redundant behaviors. I-MV-TD (Dec) slightly improves

²RiskQ and RMIX need to factorize the return’s *full* distribution into individual utilities, which tends to become unstable as the number of robots increases.

Table III: MV-FAC’s Ablation Study.

Env.	N	ζ	I-MV-TD (ϵ)	I-MV-TD (Dec)	MV-TD + MV-FAC (ϵ)	MV-TD + MV-FAC + Dec-PO
OFFICE	3	0.1	11.24	9.56	6.12	5.18
		1.0	22.15	18.30	9.45	8.06
		10.0	135.40	98.20	48.12	36.86
	4	0.1	10.85	8.92	5.65	4.84
		1.0	24.60	19.45	8.80	7.16
		10.0	152.10	112.50	42.60	30.38
	5	0.1	10.50	8.55	5.40	4.68
		1.0	26.80	21.10	8.15	6.58
		10.0	168.30	125.40	35.80	25.57

cooperation via stochastic policy updates, but lacks explicit
509 inter-robot coordination. Introducing MV-FAC significantly
510 enhances cooperation, while the ϵ -greedy policy still causes
511 instability. Finally, MV-TD+MV-FAC+Dec-PO consistently
512 achieves the best mean–std performance, combining effective
513 coordination with stable policy optimization.

6 Conclusion and Future Work

This paper formulates a risk-sensitive multi-robot search
516 problem, termed MuRMSS, characterized by an inherently
517 non-additive mean–standard deviation objective on search
518 time. To address this challenge, we propose MV-FAC, an
519 RL-based framework for MuRMSS, enabling joint mean–
520 variance estimation, consistent factorization, and decentral-
521 ized policy optimization. Extensive experiments on standard
522 benchmarks demonstrate that MV-FAC consistently achieves
523 superior mean–standard deviation performance over state-of-
524 the-art baselines. In the future, we plan to incorporate multi-
525 robot deadlock resolution mechanisms into MV-FAC under
526 risk-sensitive objectives, and to explore integrating graph
527 foundation models to improve the generalization ability of
528 MV-FAC across diverse and previously unseen environments.

References

- [Andreychuk *et al.*, 2025] Anton Andreychuk, Konstantin S. Yakovlev, Aleksandr Panov, and Alexey Skrynnik. Advancing learnable multi-agent pathfinding solvers with active fine-tuning. In *2025 IEEE/RSJ International Conference on Intelligent Robots and Systems (IROS)*, pages 10564–10571, 2025.
- [Asfora *et al.*, 2020] Beatriz A. Asfora, Jacopo Banfi, and Mark E. Campbell. Mixed-integer linear programming models for multi-robot non-adversarial search. *IEEE Robotics and Automation Letters (RA-L)*, 5:6805–6812, 2020.
- [Bone *et al.*, 2023] Sean Bone, Luca Bartolomei, Florian Kennel-Maushart, and Margarita Chli. Decentralised multi-robot exploration using Monte Carlo Tree Search. In *2023 IEEE/RSJ International Conference on Intelligent Robots and Systems (IROS)*, pages 7354–7361, 2023.
- [Calzolari *et al.*, 2025] Gabriele Calzolari, Vidya Sumathy, Christoforos Kanellakis, and George Nikolakopoulos. Reinforcement learning driven multi-robot exploration via explicit communication and density-based frontier search. In *2025 IEEE International Conference on Robotics and Automation (ICRA)*, pages 11406–11412, 2025.
- [Cao *et al.*, 2024] Xiao Cao, Mingyang Li, Yuting Tao, and Peng-Chen Lu. HMA-SAR: Multi-agent search and rescue for unknown located dynamic targets in completely unknown environments. *IEEE Robotics and Automation Letters (RA-L)*, 9:5567–5574, 2024.
- [Chen *et al.*, 2024] Jiayu Chen, Chao Yu, Guosheng Li, Wenhao Tang, Shilong Ji, Xinyi Yang, Botian Xu, Huazhong Yang, and Yu Wang. Online planning for multi-uav pursuit-evasion in unknown environments using deep reinforcement learning. *IEEE Robotics and Automation Letters (RA-L)*, 10:8196–8203, 2024.
- [Chen *et al.*, 2025] Yong Chen, Yu Shi, Xunhua Dai, Qing Meng, and Tao Yu. Pursuit-evasion game with online planning using deep reinforcement learning. *Applied Intelligence*, 55, 2025.
- [Cui *et al.*, 2021] Jianfeng Cui, Dongchang Li, Peng Liu, Jia Qin, Yuedong Ma, and Zhigang Lu. Game-model prediction hybrid path planning algorithm for multiple mobile robots in pursuit evasion game. In *2021 IEEE International Conference on Unmanned Systems (ICUS)*, pages 925–930, 2021.
- [Esfahani *et al.*, 2026] Messiah Abolfazli Esfahani, Ayşe Başar, and Sajad Saeedi. FG-PE: Factor-graph approach for multi-robot pursuit–evasion. *Robotics and Autonomous Systems (RAS)*, 195:105216, 2026.
- [Fang *et al.*, 2022] Xu Fang, Chen Wang, Lihua Xie, and Jie Chen. Cooperative pursuit with multi-pursuer and one faster free-moving evader. *IEEE Transactions on Cybernetics (ToC)*, 52(3):1405–1414, 2022.
- [Gao *et al.*, 2021] Yue Gao, Kry Yik Chau Lui, and Pablo Hernandez-Leal. Robust risk-sensitive reinforcement learning agents for trading markets. In *Reinforcement Learning for Real Life (RL4RealLife) Workshop at ICML*, 2021.
- [Gonzalez and Jaillet, 2025] Victor Gonzalez and Patrick Jaillet. Multi-drone rescue search in a large network. *European Journal of Operational Research (EJOR)*, 324:787–798, 2025.
- [Guo *et al.*, 2023a] Hongliang Guo, Zhaokai Liu, Rui Shi, Wei-Yun Yau, and Daniela Rus. Cross-entropy regularized policy gradient for multirobot nonadversarial moving target search. *IEEE Transactions on Robotics (T-RO)*, 39:2569–2584, 2023.
- [Guo *et al.*, 2023b] Hongliang Guo, Qihang Peng, Zhiguang Cao, and Yaochu Jin. DRL-Searcher: A unified approach to multirobot efficient search for a moving target. *IEEE Transactions on Neural Networks and Learning Systems (TNNLS)*, 35:3215–3228, 2023.
- [Guo *et al.*, 2025] Hongliang Guo, Qi Kang, Wei-Yun Yau, Chee-Meng Chew, and Daniela Rus. R-FAC: Resilient value function factorization for multirobot efficient search with individual failure probabilities. *IEEE Transactions on Robotics (T-RO)*, 41:3385–3401, 2025.
- [Hou *et al.*, 2024] Yukai Hou, Jin Zhao, Rongqing Zhang, Xiang Cheng, and Liuqing Yang. UAV swarm cooperative target search: A multi-agent reinforcement learning approach. *IEEE Transactions on Intelligent Vehicles (T-IV)*, 9:568–578, 2024.
- [Hu *et al.*, 2025] Kun Hu, Muning Wen, Xihuai Wang, Shao Zhang, Yiwei Shi, Minne Li, Minglong Li, and Ying Wen. PMAT: Optimizing action generation order in multi-agent reinforcement learning. In *Proceedings of the 24th International Conference on Autonomous Agents and Multiagent Systems (AAMAS)*, pages 997–1005, 2025.
- [Jiang *et al.*, 2025] Jiahui Jiang, Wang He, and Wenwu Yu. Risk-averse multi-agent reinforcement learning with distributional mean–variance formulation. In *International Conference on Artificial Intelligence and Machine Learning Research (CAIMLR)*, volume 13635. SPIE, 2025.
- [Jo and Son, 2025] Yuseung Jo and Hyoung Il Son. CBS-HT: Prioritized safe interval path-planning algorithm for heterogeneous agricultural robot team. *IEEE Access*, 13:146630–146648, 2025.
- [Knuth, 1976] Donald E. Knuth. Big Omicron and big Omega and big Theta. *SIGACT News*, 8(2):18–24, April 1976.
- [Kolling and Kleiner, 2013] Andreas Kolling and Alexander Kleiner. Multi-UAV motion planning for guaranteed search. In *Proceedings of the 12th International Conference on Autonomous Agents and Multi-Agent Systems (AAMAS)*, AAMAS ’13, page 79–86, Richland, SC, 2013. International Foundation for Autonomous Agents and Multiagent Systems.
- [Kuba *et al.*, 2022] JG Kuba, R Chen, M Wen, Y Wen, F Sun, J Wang, and Y Yang. Trust region policy optimisation in multi-agent reinforcement learning. In *Proceedings of the 10th International Conference on Learning Representations (ICLR)*, pages 1046–1072, 2022.

- 641 [Kwa *et al.*, 2020] Hian Lee Kwa, Jabez Leong Kit, and
642 Roland Bouffanais. Optimal swarm strategy for dynamic
643 target search and tracking. In *Proceedings of the 19th International Conference on Autonomous Agents and Multi-Agent Systems (AAMAS)*, pages 672–680, 2020.
644
- 645 [Lee and Lee, 2024] Seung-Mok Lee and Jeong-Uk Lee. Multi-robot formation planning in maze-like environments consisting of narrow passages using graph search. *IEEE Access*, 12:167694–167704, 2024.
- 646 [Morin *et al.*, 2022] Michael Morin, Irène Abi-Zeid, and
647 Claude-Guy Quimper. Ant colony optimization for path
648 planning in search and rescue operations. *European Journal of Operational Research (EJOR)*, 305:53–63, 2022.
- 649 [Olsen *et al.*, 2022] Trevor Olsen, Nicholas M. Stiffler, and
650 Jason M. O’Kane. Robust-by-design plans for multi-
651 robot pursuit-evasion. In *2022 International Conference on Robotics and Automation (ICRA)*, pages 10716–10722,
652 2022.
- 653 [Patil *et al.*, 2023] Indraneel Patil, Rachel Zheng, Charvi
654 Gupta, Jaekyun Song, Narendar Sriram, and Katia P. Sycara. Graph-based simultaneous coverage and exploration planning for fast multi-robot search. *ArXiv*,
655 abs/2303.02259, 2023.
- 656 [Peng *et al.*, 2025a] Qihang Peng, Hongliang Guo, Boyang
657 Li, Chih-Yung Wen, and Yaochu Jin. SMC-Searcher: Signal
658 mediated coordination for decentralized multi-robot
659 adversarial moving target search. *IEEE Transactions on Emerging Topics in Computational Intelligence (TETCI)*,
660 9(5):3399–3412, 2025.
- 661 [Peng *et al.*, 2025b] Qihang Peng, Hongliang Guo, Zhengyan
662 Zhang, Chih-Yung Wen, and Yaochu Jin. PF-MAAC: A learning-based method for probabilistic
663 optimization in time-constrained non-adversarial moving
664 target search. *Swarm and Evolutionary Computation*,
665 92:101785, 2025.
- 666 [Qiu *et al.*, 2021] Wei Qiu, Xinrun Wang, Runsheng Yu,
667 Rundong Wang, Xu He, Bo An, Svetlana Obraztsova,
668 and Zinovi Rabinovich. RMIX: Learning risk-sensitive
669 policies for cooperative reinforcement learning agents.
670 In *Advances in Neural Information Processing Systems (NeurIPS)*, volume 34, pages 23049–23062, 2021.
- 671 [Rahman *et al.*, 2022] A. Azizur Rahman, Arnab Bhattacharya, Thiagarajan Ramachandran, Sayak Mukherjee, Himanshu Sharma, Ted Fujimoto, and Samrat Chatterjee. AdverSAR: Adversarial search and rescue via multi-agent reinforcement learning. In *2022 IEEE International Symposium on Technologies for Homeland Security (HST)*, pages 1–7, 2022.
- 672 [Rashid *et al.*, 2020] Tabish Rashid, Mikayel Samvelyan, Christian Schroeder De Witt, Gregory Farquhar, Jakob Foerster, and Shimon Whiteson. Monotonic value function factorisation for deep multi-agent reinforcement learning. *Journal of Machine Learning Research (JMLR)*, 21(1):7234–7284, 2020.
- 673 [Sharma *et al.*, 2025] Vikas Sharma, Rahul Gupta, and K.R. Sharma. Swarm intelligence in robotics: Optimizing PSO
674
- 675 parameters for target search in single and multiple scenarios. In *International Conference on Mechatronics and Robotics Engineering (ICMRE)*, pages 140–144, 2025.
676
- 677 [Shen *et al.*, 2023] Siqi Shen, Chennan Ma, Chao Li, Weiquan Liu, Yongquan Fu, Songzhu Mei, Xinwang Liu, and Cheng Wang. RiskQ: risk-sensitive multi-agent reinforcement learning value factorization. In *Advances in Neural Information Processing Systems (NeurIPS)*, volume 36, pages 34791–34825, 2023.
- 678 [Sheng *et al.*, 2022] Wenda Sheng, Hongliang Guo, Wei-Yun Yau, and Yingjie Zhou. PD-FAC: Probability density factorized multi-agent distributional reinforcement learning for multi-robot reliable search. *IEEE Robotics and Automation Letters (RA-L)*, 7(4):8869–8876, 2022.
- 679 [Shree *et al.*, 2021] Vikram Shree, Beatriz Asfora, Rachel Zheng, Samantha Hong, Jacopo Banfi, and Mark Campbell. Exploiting natural language for efficient risk-aware multi-robot SaR planning. *IEEE Robotics and Automation Letters (RA-L)*, 6(2):3152–3159, 2021.
- 680 [Slumbers *et al.*, 2022] Oliver Slumbers, David Henry Mguni, Stefano B. Blumberg, Stephen Marcus McAleer, Yaodong Yang, and Jun Wang. A game-theoretic framework for managing risk in multi-agent systems. In *International Conference on Machine Learning (ICML)*, pages 32059–32087, 2022.
- 681 [Sun *et al.*, 2020] Yinjiang Sun, Rui Zhang, Wenbao Liang, and Cheng Xu. Multi-agent cooperative search based on reinforcement learning. In *2020 3rd International Conference on Unmanned Systems (ICUS)*, pages 891–896, 2020.
- 682 [Sun *et al.*, 2021] Wei-Fang Sun, Cheng-Kuang Lee, and Chun-Yi Lee. DFAC Framework: Factorizing the value function via quantile mixture for multi-agent distributional Q-learning. In *International Conference on Machine Learning (ICML)*, pages 9945–9954, 2021.
- 683 [Sutton and Barto, 2018] Richard S. Sutton and Andrew G. Barto. *Reinforcement Learning: An Introduction*. The MIT Press, second edition, 2018.
- 684 [Tan *et al.*, 2021] Aaron Hao Tan, Federico Pizarro Bejarano, Yuhan Zhu, Richard Ren, and Goldie Nejat. Deep reinforcement learning for decentralized multi-robot exploration with macro actions. *IEEE Robotics and Automation Letters (RA-L)*, 8:272–279, 2021.
- 685 [Yuan *et al.*, 2024] Shilong Yuan, Zhou He, Pengyang He, and Wei Tang. An improved ant colony optimization algorithm for multi-robot path planning under complex tasks. In *International Conference on Intelligent Robotics and Control Engineering (IRCE)*, pages 95–99, 2024.
- 686 [Zhou *et al.*, 2024a] Meng Zhou, Xinheng Wang, Chang Wang, and Jing Wang. Multi-robot cooperative target search based on distributed reinforcement learning method in 3D dynamic environments. *Drones and Autonomous Vehicles*, 1:10012, 2024.
- 687 [Zhou *et al.*, 2024b] Yinglu Zhou, Yinya Li, Andong Sheng, Guoqing Qi, and Jinliang Cong. Optimal control strategies and target selection in multi-pursuer multi-evader differential games. *Neurocomputing*, 588:127701, 2024.